RECENT RESULTS OF REFLECTOMETRY ON ASDEX-UPGRADE

M.Manso, F.Serra, I.Nunes, L. Cupido, V. Grossmann, M. Maraschek*, L. Meneses, J. Santos, A.Silva, F. Silva, P.Varela, S. Vergamota

Associação EURATOM/IST, Centro de Fusão Nuclear, Instituto Superior Técnico, 1096 Lisboa Codex, Portugal

**Max-Planck-Institut fur Plasmaphysik, EURATOM Association, D-85748 Garching, Germany*

I. Introduction

Reflectometry is well known to be very sensitive to plasma density fluctuations. This characteristic is used to study plasma modes and turbulence from probing signals with fixed frequencies. When the frequency of the launched waves is swept over a certain frequency range, the reflected signals exhibit a much more complex response due to the reflections at different plasma layers and different time instants. The interference signal should, in principle, exhibit a dominant frequency corresponding to the group delay associated with the distance between the launching antenna and the reflection layer, which is the relevant data for density profile evaluation.

In the experiments, however, the secondary peaks due to the plasma fluctuations can become significant subtracting a large part of the energy from the main peak, which thereby decreases or even vanishes. Another effect is a frequency shift of the main component associated with local fast profile deformations. Due to the above reasons the distance information is not easy to interpret when the level of plasma fluctuations is high.

The study of the plasma response in broadband frequency operation concentrated on the obtention of the main peak and many techniques have been developed to filter the unwanted components. In comparison litle work has been done to understand the remaining part of the signal.

There are strong reasons, however, that advise the analysis of the complete plasma response. It permit to complement the results given by the fixed frequency measurements and to enlight the meaning of the average density profile. This knowledge can certainly lead to new developments of the methods of analysis to extract the group delay and will improve the accuracy of the inverted profiles.

Here we present some recent results about plasma fluctuations obtained with FM-reflectometry on ASDEX-Upgrade. They demonstrate the rich content information of both the fixed frequency and broadband signals and suggest that they can be used in a complementary way.

II. Fixed frequency measurements

The ASDEX Upgrade plasma was probed with several fixed frequencies in the range: 18-70 GHz, corresponding to reflecting densities between 0.4 and 6.5×10^{19} m^{-3} [1]. The plasma was probed at a rate of 1 μs (1 MHz sampling frequency). Taking into account the wavelengths involved and the geometry of the launching antennas, the radial turbulence wavenumber selected at the cut-off layer is <1-2 cm^{-1} (spatial width of the cut-off: 2-3 cm), and the poloidal turbulence wavenumber is $\sim 1.5<k<8.5$ cm^{-1}.

(i) Study of turbulence during the L-H transition

In these experiments the reflectometry channels were operated at fixed frequencies of 22.7, 31.7 and 45.7 GHz to probe plasma densities n_e: 0.64, 1.24 and 2.58×10^{19} m^{-3}, respectively. Measurements were performed in shot #8595 with unfavourable ∇B drift direction (away from the X-point) where H-mode is attained through ctr-NBI (Fig 1(a)), as observed in the D_α signal shown in Fig. 1(b). The temporal evolution of turbulence at the three density layers can be inferred from the power spectra contour plots in figures 1(c) – (e), obtained with a sliding FFT technique [2]. At the L-H transition ($t \sim 1.704$ s), the fluctuations are reduced in all channels both at low- (figures 1(c) and (d)) and high-field sides (figure 1(e)), coinciding with the drop of the D_α signal. For the innermost layer ($n_e \sim 2.6 \times 10^{19}$ m^{-3}), well inside the separatrix ($n_{es} \sim 1.2 \times 10^{19}$ m^{-3}) at the onset of NBI, a broadening of the frequency spectrum occurs correlated with the NBI. The frequency

bandwidth increases during the L-phase, as the probed layer is moving radially outwards towards the gradient region of the profile with increased turbulence; with high heating power (5 MW, after 1.65 s) the frequency range increases abruptly, reaching ~ 300 kHz just before the transition. After ~ 1.67 s the fluctuations in the range ~ 30-100 kHz are reduced and the high-amplitude fluctuations are displaced to higher frequencies. Although this could indicate an increase of density fluctuations it is more likely to be due to a Doppler shift induced by an E × B poloidal velocity. In fact, the frequency-integrated power obtained from the turbulent spectra is approximately constant in the interval 1.67-1.703 s. An increase of the E × B velocity inside the separatrix is consistent with the observed growth (as inferred from changes in the fluxes of ripple-trapped charge-exchange neutrals [3]) of the radial electric field (E_r) at the edge, before the L-H transition, preceding the density profile build up during the H-phase.

(ii) Improved core confinement discharges with H-mode edge

In this section a discharge is analysed where an internal transport barrier (ITB) coexists with an edge H-mode barrier [4]. Fig. 2 shows for # 12031 the temporal evolution of: (a) neutral beam power; (b) central T_i; (d) integrated power spectra from reflectometry at a layer with $n_e \sim 2.8 \times 10^{19}$ m^{-3}; the power spectra of reflectometry (from contour plots of sliding FFT), at (e) $n_e \sim 2.8 \times 10^{19}$ m^{-3} and (f) $n_e \sim 0.8 \times 10^{19}$ m^{-3}, located respectively at r/a ~ 0.6 and close to the separatrix. At the inner layer, the fluctuation level decreases abruptly at t ~ 1.07 s, before the 2nd beam starts, coinciding with the increase of T_e and the confinement factor, and preceeding (by ~ 50 ms) the reduction at the edge at the L-H transition, occuring at t ~1.12s. This indicates that the confinement starts to improve at the core during the current ramp phase, before the edge H-mode barrier is formed. After 1.18 s the observed oscillations at the outer layer are correlated with the turbulence due to ELMs.

Prior to the improvement in the core, a shift of the turbulence spectrum to higher frequencies is observed indicating an increase of the plasma rotation. This is also seen at the edge prior to the L-H transition and it is a typical feature found in H-mode regimes with or without ITBs. At the formation of the edge barrier, the power integrated spectra

attains a minimum level which may be explained be explained by a further increase of plasma core rotation due to the formation of the edge barrier.

III. Broadband measurements

Broadband measurements are obtained by sweeping continuously the frequency of each reflectometer channel. In broadband operation the complete plasma is probed in 20 μs by the simultaneous operation of the different channels (full band) located both at the low and high field sides. The minimum interval between consecutive sweeps is 20 μs and it can be programmed before each shot according to the type of study to be performed, taking into account that the maximum number of measurements possible with the present data acquisition system is 720.

1. Density profiles in discharges with Laser ablated impurities

Broadband measurements were performed in discharges where edge cooling pulses are produced by injection of impurities by means of Laser-Blow-Off (LBO). In such conditions a fast increase of the electron temperature in the center is observed and the confinement is improved [5]. As these low densities discharges have a reduced level of fluctuations, the distance information is easy to obtain from the reflected signals. This clear cases are useful to evaluate the capability of the reflectometer diagnostic to measure the density profile and serve as a reference to analyse more difficult situations.

In Fig. 3 it is shown the evolution of the line integrated density in ASDEX Upgrade shot #11711 obtained from the DCN interferometer and the vertical lines corresponding to the sampling times of reflectometry. In this discharge the cold pulse was produced by injection of Si by means of LBO (between 3.75s and 5.5s).

The spectrogram of the interference signals (see Fig. 4) resulting from the interference between the reflected and reference signals clearly show a dominant component whose frequency (interference frequency f_B) increases with the probing microwave frequency (F). In Fig. 4 two spectrograms are shown obtained respectively at probing instants t_1 and t_9. In the horizontal axis we plot the group delay (t_g) which can be directly related to f_B by: $t_g = f_g \left(\frac{dF}{dt}\right)^{-1}$. Plasma density n_e, which is proportional to the probing

frequency F, is represented in the vertical axis. The solid line in each spectrogram gives the evolution of the group delay ($t_g \propto f_B$) and is obtained automatically using a best path algorithm [6]. The t_g (F) data after Abel inversion permits to obtain the density profiles, shown in Fig. 4 for the time instants corresponding to the two spectrograms.

Several density profiles were measured automatically both at the low and high field sides as shown in Fig. 5. After the S_i Laser Blow-Off (starting at t = 3.75s) a steepening of the density profiles is observed at both sides (measured after $t \cong 4.41$s) in agreement with the improvement of confinement. The density profiles that are represented in major radius R (m) exhibit lower density gradients at the HFS than at the LFS due to the larger spacing of the magnetic field surfaces at the inner side. In Figs. 6 it is depicted the density profiles from the HFS after being mapped into the LFS (dashed lines) by plotting the density along the corresponding magnetic field surfaces. They are in good agreement with the LFS profiles (solid lines), the small shifts observed can be due to the initialization procedure and also to some small incertainties related to the evaluation of the flux surfaces. The fact that density profiles measured with different reflectometer channels at the LHS and HFS shows the same temporal evolution and agree well when they are ploted in poloidal coordinates is a strong evidence of the good results given by the reflectometry system.

2. Profile deformations due to rotating modes

The line corresponding to the evolution of the group delay versus probing frequency F (or density) is very often distorted in one or several frequency ranges. Here we present an example where the distortions are due to magnetic activity.

The spectrograms in Fig. 7 were obtained in ASDEX Upgrade shot #11694 with optimized triangularity and neutral beam heating. They exhibit a perturbation in the frequency region 35-40 GHz although the energy remains concentrated around the main peak. During the probing intervals an MHD $m = 2$, $n = 1$ mode is present as inferred from magnetic data (Fig. 10 a). This means that the mode is seen as "frozen" by reflectometry (the region 35-40 GHz is swept in $\Delta t \leq 5\mu s$ while the typical period of rotation is 200 μs). The observed deformations of the group delay correspond to density plateaus in the density profiles (see Fig. 8). The fact that the flattening of the profile is

observed when the MHD activity appears and its growth when this activity increases (for t = 2.78632s, as measured by the magnetic coils) clearly indicates that the observed profile deformations are related to the magnetic modes. It should be noted that the main mode is located close to the separatrix and therefore the observed density plateaus should be due to sattelite modes. These also have impact on the fixed frequency signals, as shown (for t: 2.5 s - 3.0 s) in Fig. 9 where the mode (with f starting ~ 5 kHz) and its harmonics are clearly observed for $n_e \sim 2.2\times10^{19}$ m^{-3}, in good agreement with the temporal dependence of the magnetic signals.

3. Density profile fluctuations during ELMS

During ELMs, coinciding with the rise of the D_α signal, the reflected signals exhibits a rather broad spectra and in many situations it is difficult or even impossible to track any line due to distance. This is the case of the spectrograms shown in Fig.10, obtained during an ELM type I in ASDEX Upgrade shot #11557, respectively at the peak of the ELM (t = 2.01845s) and shortly after (t = 2.01875s). In order to understand the meaning of the observed frequency pattern, we mapped in Fig.11 the automatically extracted group delay curves (which in some sweeps are not meaningful for profile evaluation) versus time (multi sweeps) and density. Also represented is the colour code corresponding to the values of group delay. Localized density perturbations are observed which follow the evolution of the D_α signal (seen in the Fig. 11 for two consecutive ELMs). At the peak of the second ELM the complete profile is disturbed. In the second instants the fluctuations had already decreased. The mapping of Fig. 11 shows an increase of the group delay (t_g) for densities higher than $n_{e\alpha} \sim 3\times10^{19}$ m^{-3} (which means a displacement of the reflecting layers away from the antenna) and a decrease of the group delay for densities lower than $n_{e?}$ (related to a displacement of the reflecting layers towards the antenna). Both displacements indicate a flatenning of the profile with a "turning point" around $n_{e\alpha}$, as depicted in Fig. 12. The "turning point" seems to be located close to the separatrix. Following the decrease of the D_α signal, and in the same time scale, the steep density profile typical of the H regime is recovered.

A similar study was performed in the same shot #11557 when type III ELMs occur. In this case a different pattern is observed (as seen in Fig.13) where the local density

movements are not pronounced as in the case of type I ELMs. This difference in behaviour is in agreement with well known characteristics of both type of ELMs [7]. In fact, type I ELMs occur when the edge pressure gradient reaches the ideal ballooning instability limit, leading to the H-mode barrier degradation and therefore a drastic change of the profile. On the contrary, during the type III ELMy H-mode the edge pressure gradient is significantly lower, as well as the level of fluctuations and the modifications of the profile.

4. Concluding remarks

Here we present results about the plasma fluctuations in ASDEX Upgrade obtained with both fixed frequency and broadband measurements. It is demonstrated that in addition to the standard measurements with fixed frequency, the broadband signals contain also valuable information about the plasma fluctuations, namely about magnetic modes and local profile deformations associated with type I and type III ELMs.

On the other hand, the frequency components due to the fluctuations poses great difficulties to density profile evaluation and therefore they must be understood. In a previous work it was made a first atempt to correlate the signals perturbations with some physical plasma parameters [8]. Our present study is a further contribution to enlight this problem aiming at improving the evaluation of the average density profile.

References

[1] A. Silva et al., Rev. Sci. Instruments, 67 (12) (1996).

[2] J. Santos et al., III Reflectometry Workshop for Fusion Plasmas, Madrid, (1997).

[3] W. Herrmann et al., Phys. Rev. Lett., 4401 (1995)

[4] R. Neu et al., 26th EPS Conf. on Contr. Fusion and Plasma Physics, Maastricht, Vol 23J, 1413 (1999)

[5] R. Wolf et al., IAEA Conf. Jokohama (1998).

[6] P. Varela et al., this Workshop

[7] W. Suttrop et al., PPCF39, (1997) 2051.

[8] Clairet et al., III Reflectometry Workshop for Fusion Plasmas, Madrid, (1997).

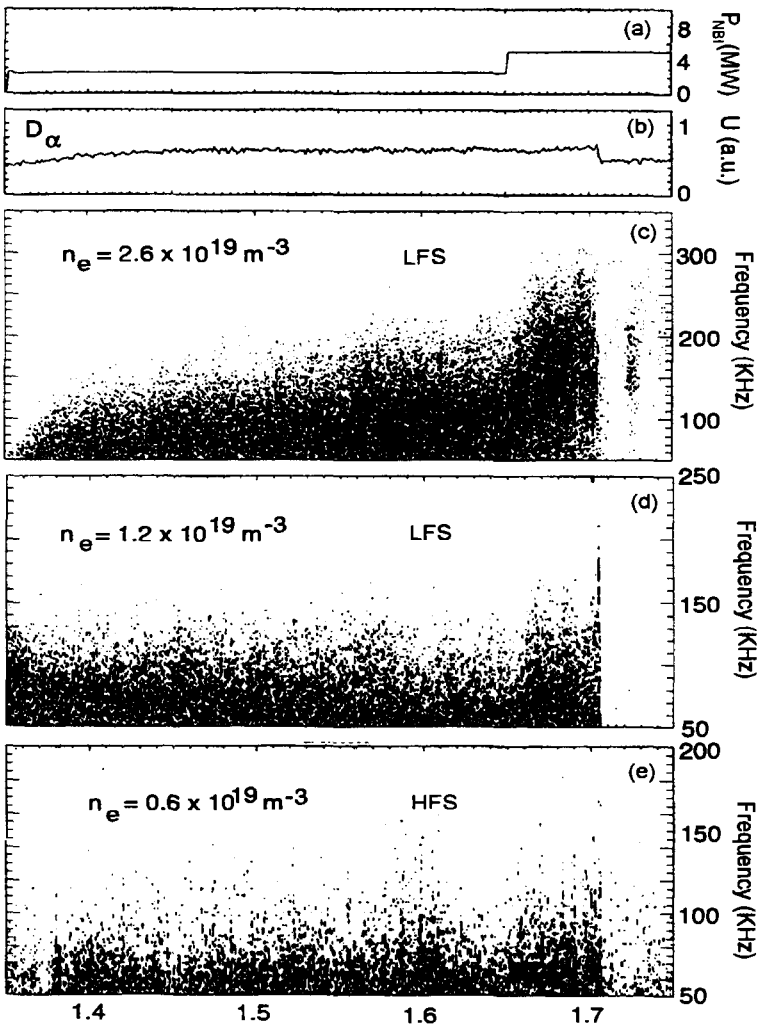
(a)
8
4
0
P_{NBI}(MW)
D_α
(b)
1
0
U (a.u.)
$n_e = 2.6 \times 10^{19}\ m^{-3}$
LFS
(c)
300
200
100
Frequency (KHz)
$n_e = 1.2 \times 10^{19}\ m^{-3}$
LFS
(d)
250
150
50
Frequency (KHz)
$n_e = 0.6 \times 10^{19}\ m^{-3}$
HFS
(e)
200
150
100
50
Frequency (KHz)
1.4
1.5
1.6
1.7

Fig. 1

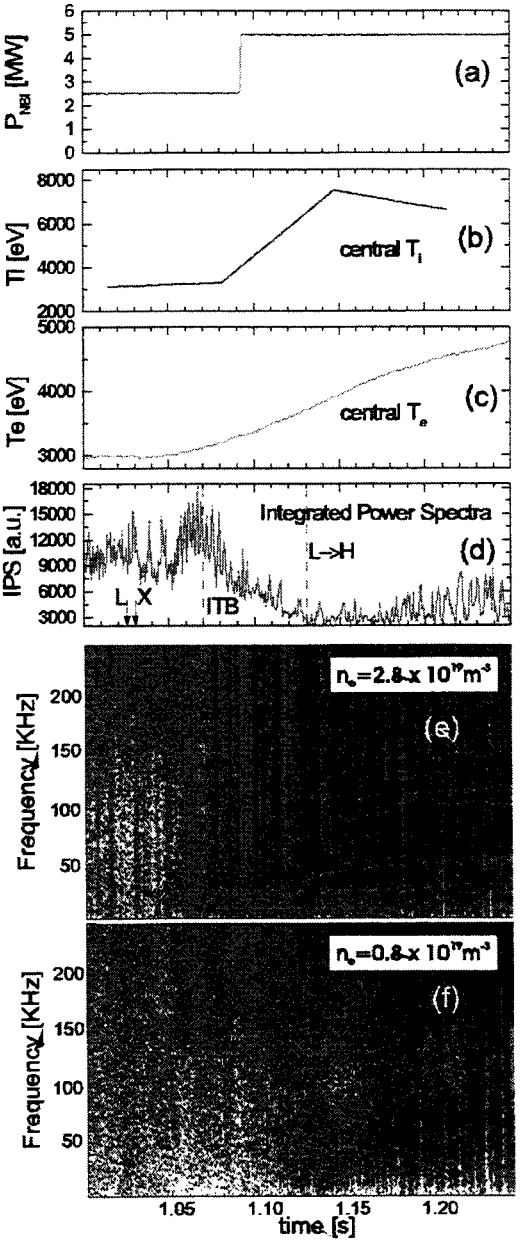
P_NBI [MW]
(a)
Ti [eV]
central T_i
(b)
Te [eV]
central T_e
(c)
IPS [a.u.]
Integrated Power Spectra
L->H
(d)
L
X
ITB
n_e=2.8-x 10^19m^-3
(e)
Frequency [KHz]
n_e=0.8-x 10^19m^-3
(f)
Frequency [KHz]
time [s]

Fig. 2

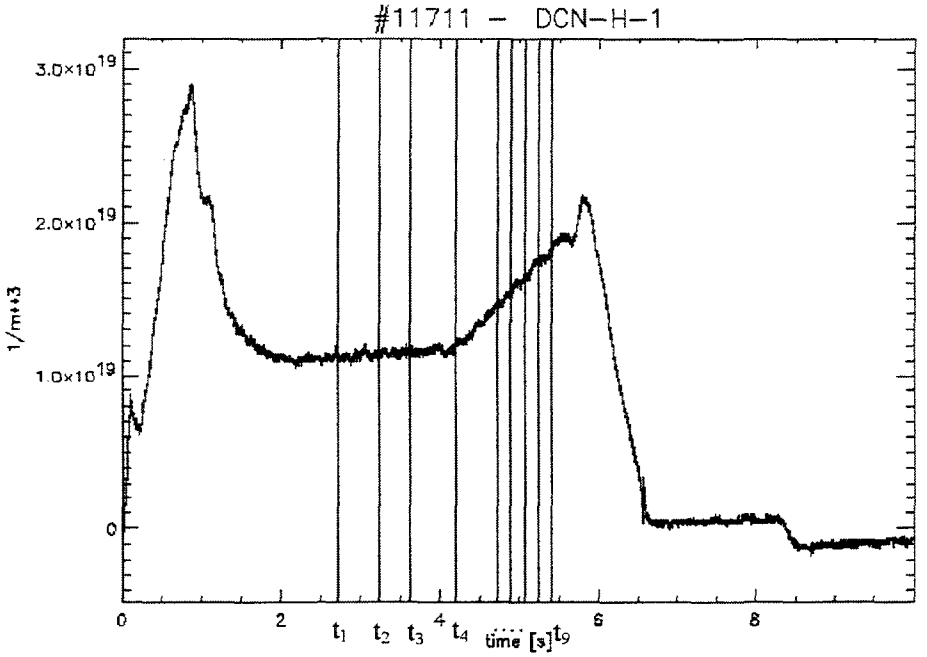
#11711 – DCN–H–1
3.0x10^19
2.0x10^19
1.0x10^19
0
1/m**3
0
2
4
6
8
time [s]
t1 t2 t3 t4 t9

Fig. 3

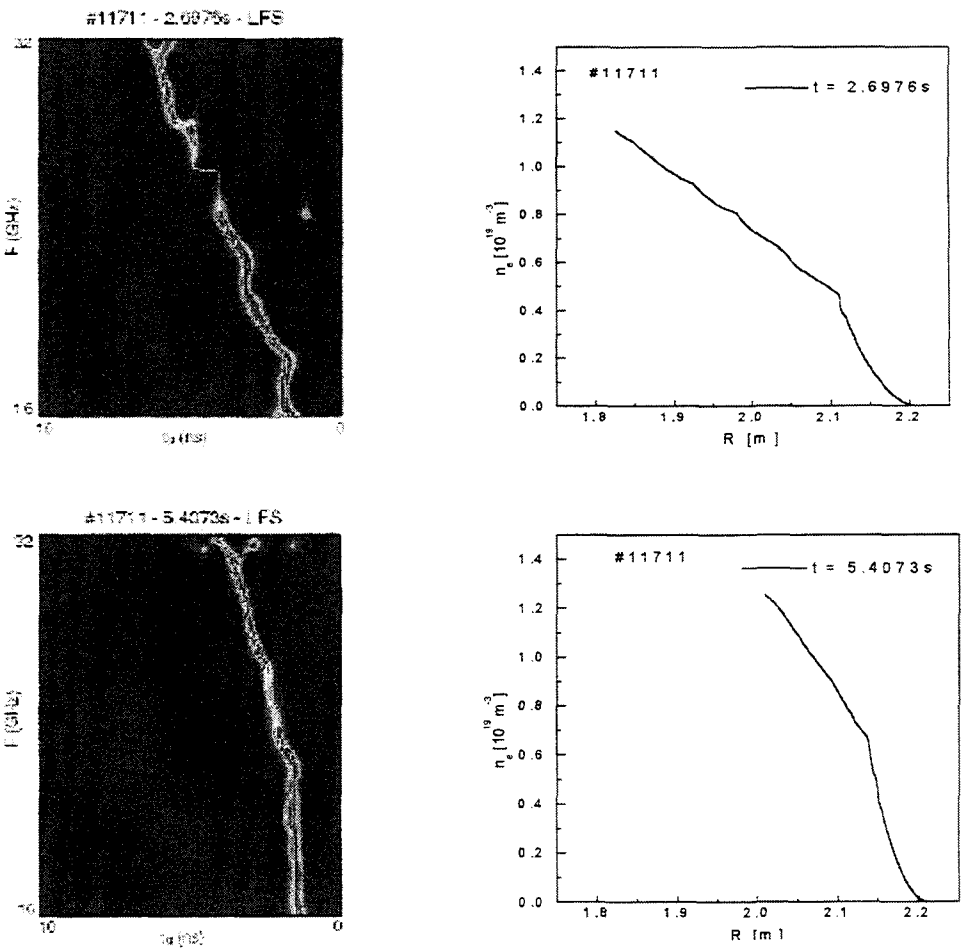
#11711 - 2.697s - LFS
#11711
t = 2.6976s
n_e [10^19 m^-3]
R [m]
#11711 - 5.4073s - LFS
#11711
t = 5.4073s
n_e [10^19 m^-3]
R [m]

Fig. 4

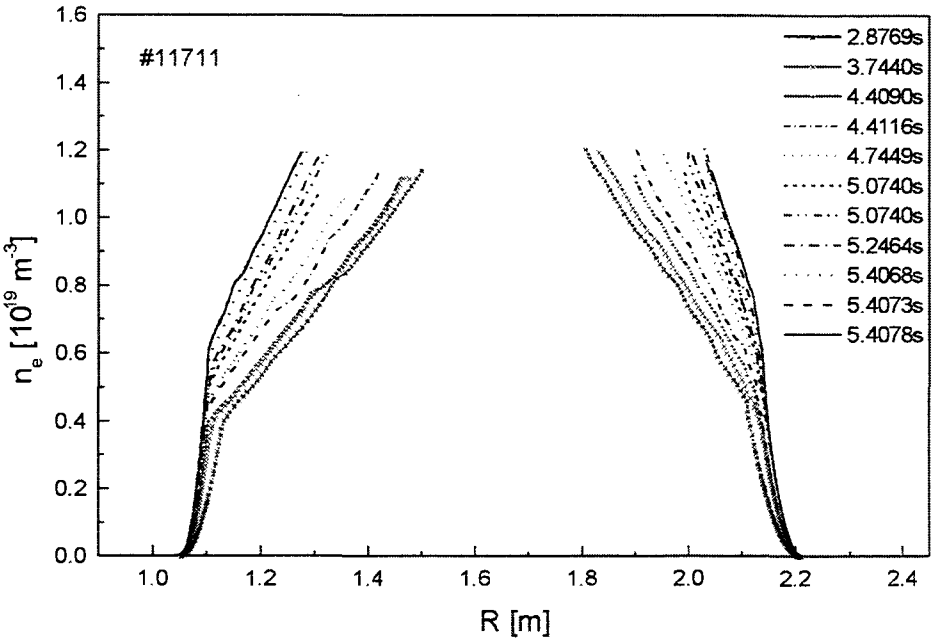
#11711
2.8769s
3.7440s
4.4090s
4.4116s
4.7449s
5.0740s
5.0740s
5.2464s
5.4068s
5.4073s
5.4078s
n_e [10^{19} m^{-3}]
R [m]

Fig. 5

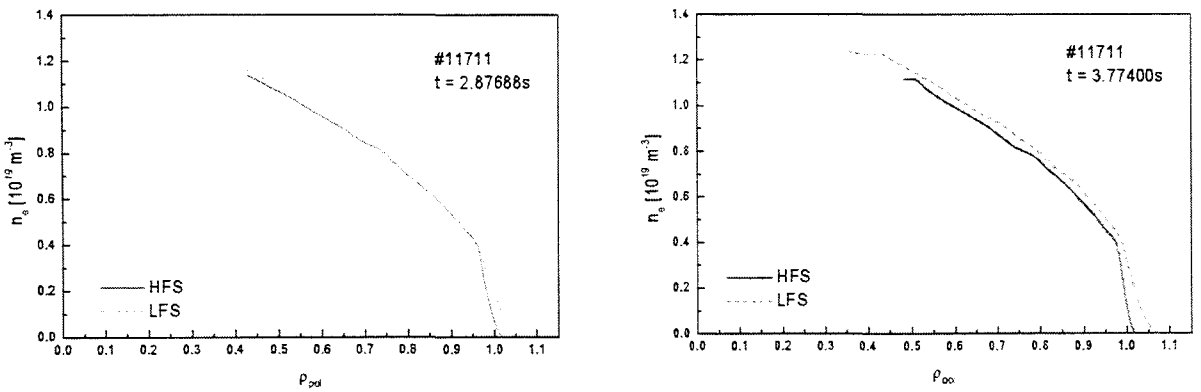
#11711
t = 2.87688s
HFS
LFS
n_e [10^{19} m^{-3}]
ρ_{pol}
#11711
t = 3.77400s
HFS
LFS
n_e [10^{19} m^{-3}]
ρ_{∞}

Fig. 6

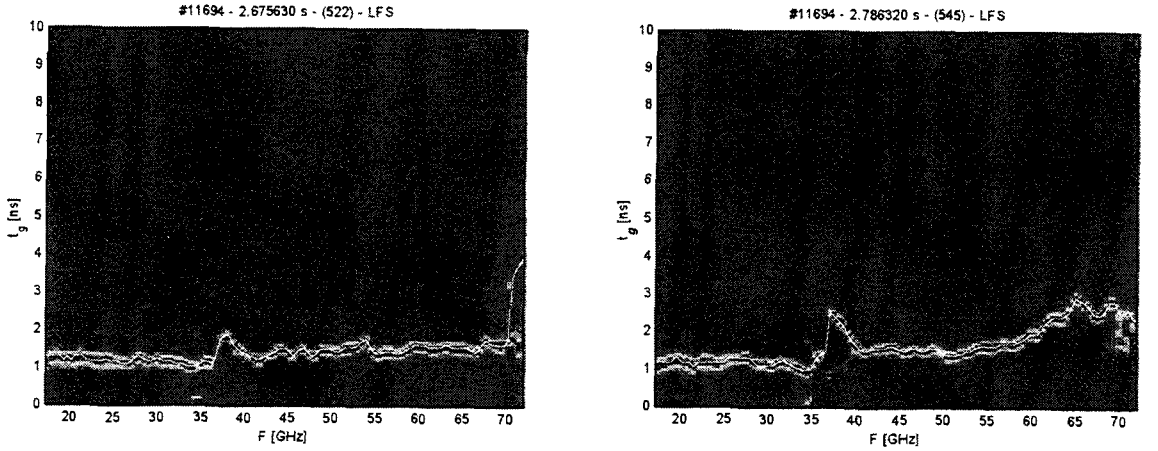
#11694 - 2.675630 s - (522) - LFS
#11694 - 2.786320 s - (545) - LFS
t_g [ns]
F [GHz]

Fig. 7

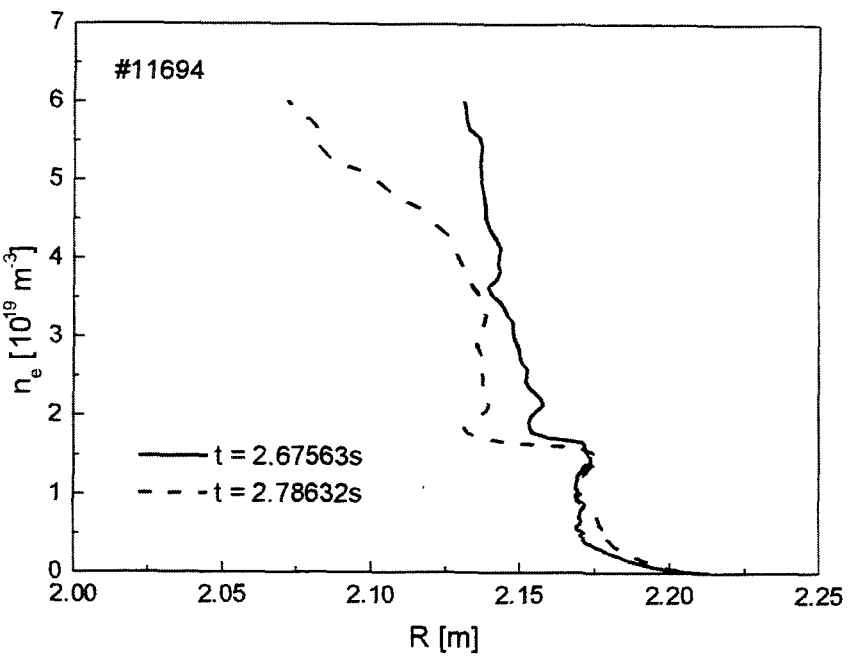
#11694
t = 2.67563s
t = 2.78632s
n_e [10^19 m^-3]
R [m]

Fig. 8

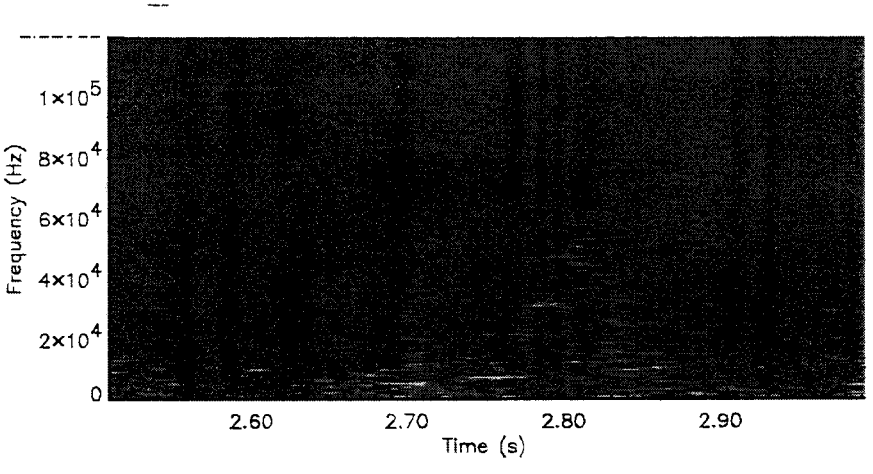

Fig. 9

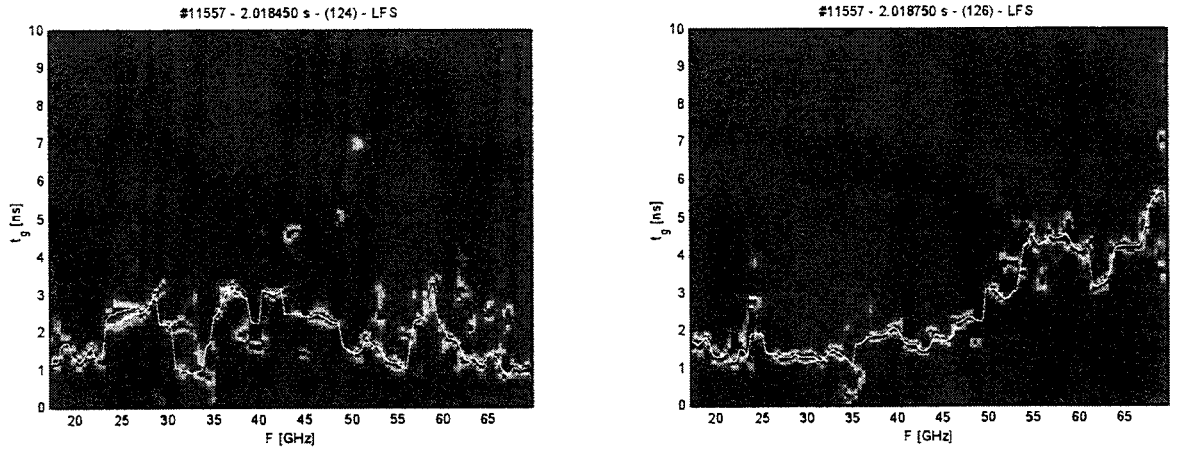
#11557 - 2.018450 s - (124) - LFS
#11557 - 2.018750 s - (126) - LFS
t_g [ns]
F [GHz]
0
1
2
3
4
5
6
7
8
9
10
20
25
30
35
40
45
50
55
60
65

Fig. 10

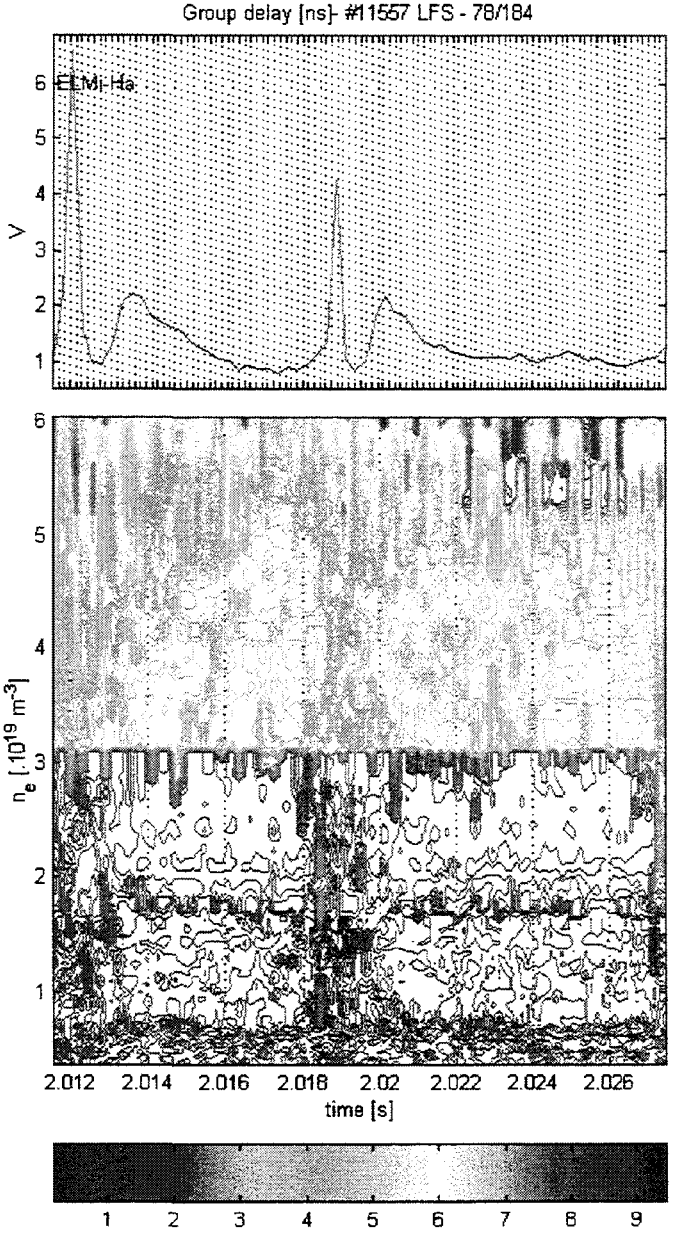
Group delay [ns]- #11557 LFS - 78/184
ELMi-Ha
V
n_e [.10^{19} m^{-3}]
time [s]
2.012
2.014
2.016
2.018
2.02
2.022
2.024
2.026

Fig. 11

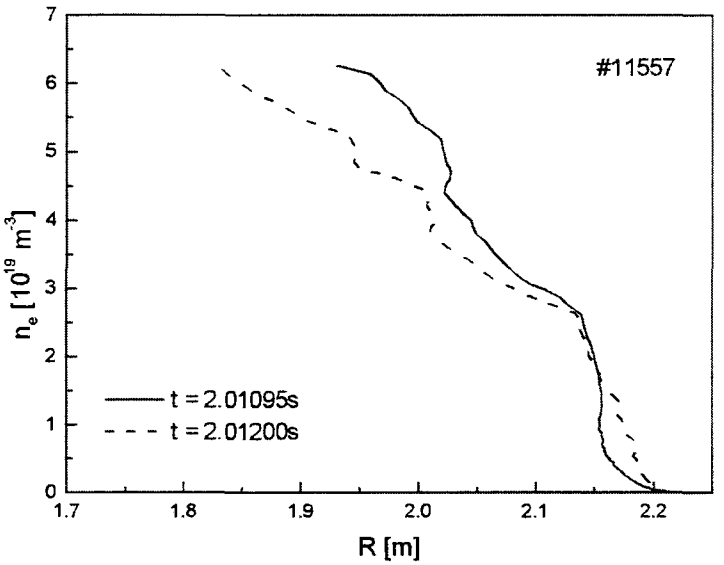
#11557
t = 2.01095s
t = 2.01200s
n_e [10^{19} m^{-3}]
R [m]
0
1
2
3
4
5
6
7
1.7
1.8
1.9
2.0
2.1
2.2

Fig.12

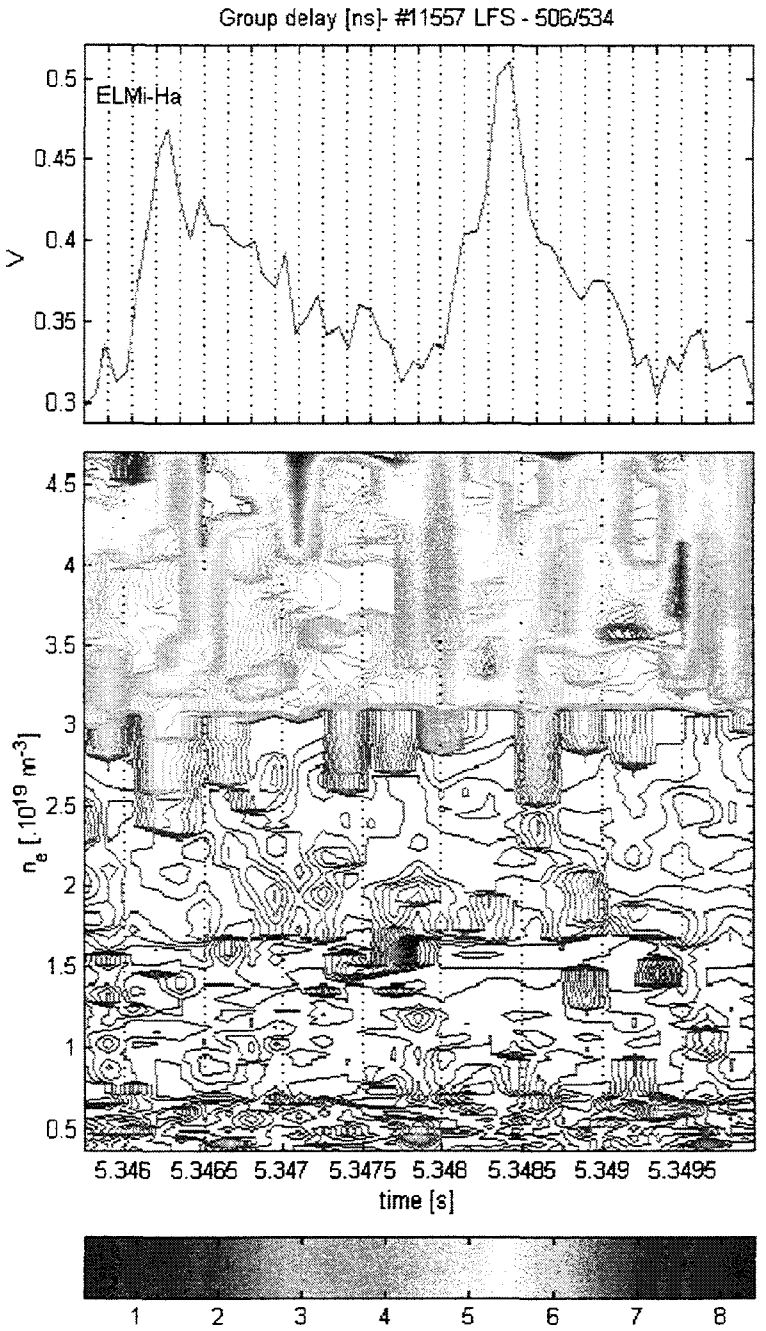
Group delay [ns]- #11557 LFS - 506/534
ELMi-Ha
V
0.5
0.45
0.4
0.35
0.3
n_e [10^{19} m^{-3}]
4.5
4
3.5
3
2.5
2
1.5
1
0.5
5.346 5.3466 5.347 5.3475 5.348 5.3485 5.349 5.3495
time [s]
1 2 3 4 5 6 7 8

Fig. 13